

Threshold adaptation and XOR accumulation algorithm for objects detection

Hasan Thabit Rashid Kurmasha^{1,2}, Israa Hadi Ali²

¹Computer Department, Education College for Women, University of Kufa, Najaf, Iraq

²Software Department, Information Technology College, University of Babylon, Hilla, Iraq

Article Info

Article history:

Received Jun 3, 2021

Revised Dec 28, 2021

Accepted Jan 31, 2022

Keywords:

Adaptive thresholding
background subtraction
Initial motion field
Noise removal
Video processing

ABSTRACT

Object detection, tracking and video analysis are vital and energetic tasks for intelligent video surveillance systems and computer vision applications. Object detection based on background modelling is a major technique used in dynamically objects extraction over video streams. This paper presents the threshold adaptation and XOR accumulation (TAXA) algorithm in three systematic stages throughout video sequences. First, the continuous calculation, updating and elimination of noisy background details with hybrid statistical techniques. Second, thresholds are calculated with an effective mean and Gaussian for the detection of the pixels of the objects. The third is a novel step in making decisions by using XOR-accumulation to extract pixels of the objects from the thresholds accurately. Each stage was presented with practical representations and theoretical explanations. On high resolution video which has difficult scenes and lighting conditions, the proposed algorithm was used and tested. As a result, with a precision average of 0.90% memory uses of 6.56% and the use of CPU 20% as well as time performance, the result excellent overall superior to all the major used foreground object extraction algorithms. As a conclusion, in comparison to other popular OpenCV methods the proposed TAXA algorithm has excellent detection ability.

This is an open access article under the [CC BY-SA](https://creativecommons.org/licenses/by-sa/4.0/) license.



Corresponding Author:

Hasan Thabit Rashid Kurmasha

Computer Department, Education College for Women, University of Kufa

Najaf, Iraq

Emails: hasan.th.kurmasha@student.uobabylon.edu.iq; hasant.kurmasha@uokufa.edu.iq

1. INTRODUCTION

Changes in scene and motion detection are two basic steps that play an essential and guiding role in simple and complex environments, where most outdoor surveillance videos are recorded [1]–[6]. However, the variation of the static background in some unfamiliar designs still make the mission of correctly extracting the foreground from the background a widely occurring challenge in surveillance video analysis [7]–[11]. Background subtraction is a necessary task in video applications such as surveillance to track, index, retrieve, and capture the essential metadata of people, cars, and other different moving objects either in real-time or off-time [12]–[16]. It is a starting point for higher processing tasks of video systems such as object identification, detection, and tracking over video sequences in recent applications and researches [17]–[21]. It is stated that many background models require the adjustment of initial frames to upgrade the background without any movement over time. Yet, such a hypothesis does not always remain true due to the dynamicity features in packed scenario backgrounds, and therefore other aspects need to be addressed. Over years, numerous background subtraction models have been suggested and established using different techniques, meanwhile their performance remains a gap, being generally based on objective and subjective

measures [22], [23]. In [24] the MOG2 model is proposed by using Gaussian mixture likelihood density and recursive equations to upgrade the factors and select the suitable amount of pixel components of objects. Moreover, the K-nearest neighbours (KNN) was proposed [25] to analyze the pixel-level background subtraction and offer a modest non-parametric adaptive density estimation method. Method in [26] made use of the Kalman filters and Gale–Shapley matching granulated metrial gland (GMG) in association with estimating the background, Bayes decision rule, and solution estimation to many objects tracking over active statistics. In [27], the adaptive local singular value decomposition (SVD) binary form as local similarity binary pattern (LSBP) feature is proposed. Its work is based on small areas that are in a given frame and tends to improve the detection process when illumination changes occur, such as noise and shadows. In [28], a speed computation algorithm of object detection is proposed which first removes noisy pixels and then applies some adaptive thresholds to catch moving objects as a foreground extraction. However, based on [29]–[33], even they propose new techniques but the problem of separating noisy background pixels in an outdoor environment remains present. The proposed threshold adaptation and XOR accumulation (TAXA) algorithm works based on how much information is available that surrounds each pixel; this information can decide whether the pixel belongs to the foreground or background; the decision is made according to the novelty use of XOR-theory for crucial adaptive thresholds of statistic techniques as shown in section 3 with detail. Section 2 presents a review of the popular related works and explains the objective and subjective measures and the weaknesses in such prominent methods. Section 4 discusses the algorithm results as compared to the alternative prominent methods, and section 5 states the conclusion of the proposed work.

2. EVALUATION MEASURES AND WEAKNESSES IN TECHNIQUES

2.1. Objective measures

The measurement of precision (quality) is the pixels ratio of the retrieved pixels as (1). It was used to assess recently the preliminary extraction techniques objectively. The precision measurement is used in particular to specify the appearance relationship between moving object and the small spread pixels which may be noisy details rather than objects in frame. It computed based on sufficient criteria namely the ground truth frame, true positive (TP), false positive (FP), true negative (TN), and false negative (FN) pixels. On the opposite, the subjective evaluation is released based on human vision observations of resulted frames. For such a tested frame, TP includes the pixels that truly represent a moving object's body and are eventually considered as foreground correctly, whereas FP involves the pixels that are in fact part of the background but are falsely identified as a moving object's body, and thus considered as foreground by mistake. TN concerns the pixels that truly represent the background and are correctly considered as background, meanwhile FN involves the pixels that are actually part of the foreground but are falsely identified as background. The ground truth frame is the frame that has optimal specifications for measuring (separate fixed background objects than moving foreground objects correctly without any noise details).

$$Precision = \frac{TP}{TP+FP} \quad (1)$$

2.2. Weaknesses in techniques

Many of the studies mentioned above claim that they subjectively have overcome many unexpected changes in indoor and outdoor lighting and noisy backgrounds (based on their findings). The performance of recent techniques OpenCV and other libraries is remarkably weak. See the following finding were the original frame No.847.jpg [33] is described in Figure 1(a), the ground truth in Figure 1(b), the MOG2 result in Figure 1(c), the KNN result in Figure 1(d), the GMG result in Figure 1(e), and the LSBP result in Figure 1(f).

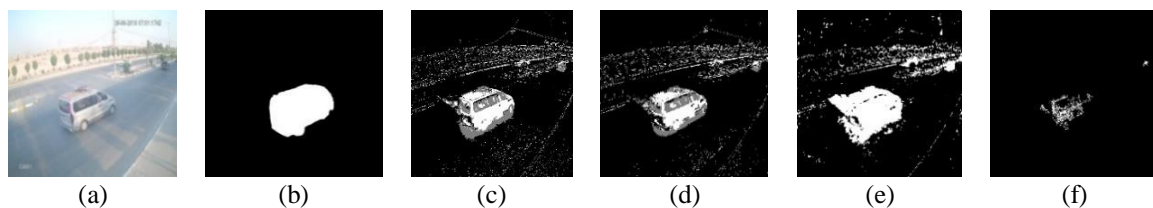


Figure 1. Results of applying the foreground moving objects extraction methods using frame No.847.jpg of recorded video (11 FPS) on 7:00 AM, (1920×1080) frame size of [33] (a) original frame, (b) ground truth, (c) MOG2, (d) KNN, (e) GMG, and (f) LSBP

The performance of the distinctive object pixels from the background pixels based upon a subjective evaluation of the Figure 1 is differs. The noisy white pixels are spreading into the background (i.e. false positive FP). They should be removed or undiscerned as object pixels. The actual white pixels of the object have. However, black pixels within the object body (i.e. false negative (FN)).

3. PROPOSED METHOD

The present study proposes the hybrid application of statistical techniques (median, Gaussian and median) after initializing, updating, and using average technique for each frame. The medium and Gaussian are therefore used to blur every frame to produce a place to remove noise as the first stage. In the second stage, the first step of extraction is performed using many adaptive Gaussian, mean, Canny edge, and pixel intensity thresholds. Finally, to merge the results threshold frames, the novel XOR-bitwise, AND, and OR operations will decide on the final separation of the pixels into the foreground and the background. Figure 2 shows the steps of the TAXA algorithm being proposed.

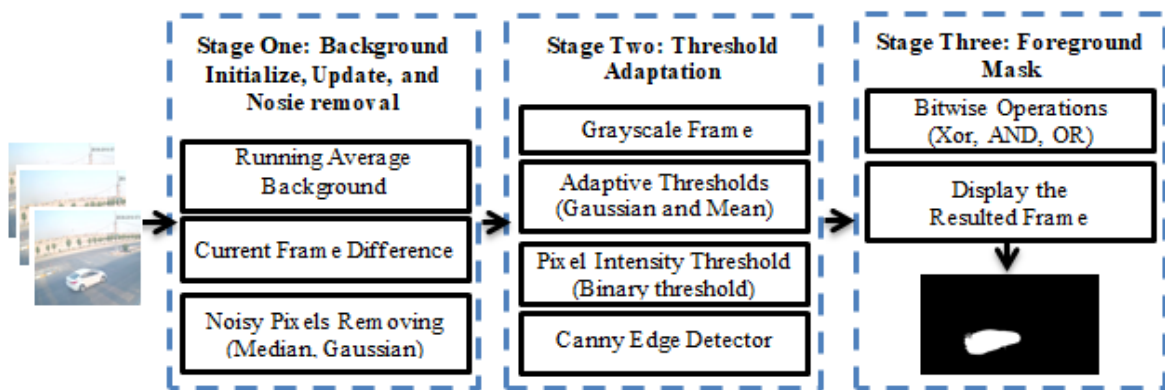


Figure 2. The proposed TAXA diagram

In stage one, the first frame is considered as background using the running averaging technique to initialize the background and updating each next frame continuously as (2):

$$Aver(r, c) = (1 - \alpha) \times Aver(r, c) + \alpha \times frame(r, c) \quad (2)$$

where, $Aver(r, c)$ is an accumulator buffer as (R, G, and B) frame's channels that compute the weighted amount of input and accumulator. The resulting turns out to be a running average of frames sequences. α (Alpha) is a learning factor value ranged (0 to 1) that brings up-to-date the speediness regulation (time spent for past frames to be unremembered by the accumulator buffer) as in Figure 3(a) for the original frame No. 1.jpg and its running average, Figure 3(b) for the original frame No. 56.jpg and its running average, Figure 3(c) for the original frame No. 90.jpg and its running average, and Figure 3(d) for the original frame No. 191.jpg and its running average.

The absolute difference $Diff(r, c)$ is calculated between both the current frame $CF(r, c)$ and the running averaging $Aver(r, c)$ buffer, which form the background as (3) while in (4), the salt-and-pepper noise is eliminated using the median mask $medBlur$ (which has a better influence) by (3×3) aperture size for the absolute difference frame.

$$Diff(r, c) = |CF(r, c) - Aver(r, c)| \quad (3)$$

$$Bf(r, c) = medBlur(Diff(r, c), 9) \quad (4)$$

The Gaussian noise is removed to the $Bf(r, c)$ by Gaussian filter which makes use of $(k \times k)$ size aperture selected through experimental results as (5).

$$Frame(r, c) = Gaussien(Bf(r, c)) \quad (5)$$

It should be observed that median filters and Gaussian filters have a point view; the center location values may not derive (not originate) from the pixel values in the source frame when the median filter's location values are derived from the original pixel values of the source frame. So balanced operations need to be applied and block sizes selected according to the experimental findings. The programming tests indicate that the process of removing noise in each pure channel data (R, G, and B) results in higher performance before it is converted to a gray channel. Then, in stage two; the colored frame is converted to grayscale frame $Gray(r, c)$ as in (6).

$$Gray(r, c) = R \times 0.299 + G \times 0.587 + B \times 0.114 \quad (6)$$

The adaptive threshold of cross-correlation is calculated with a Gaussian window ($k \times k$) for the surrounding area of pixel location (r, c) minus a constant C , using the default standard deviation of the window in (7):

$$Th1 = \begin{cases} 0 & \text{if } Gray(r, c) > T(r, c) \\ \text{maxValue} & \text{otherwise} \end{cases} \quad (7)$$

where $T(r, c)$ is the adaptive Gaussian threshold value, individually computed for each pixel as a mean of Gaussian ($k \times k$) surrounding pixel area (r, c) minus the constant C . MaxValue is the highest grayscale value is (255). In (8), the adaptive mean threshold is calculated using a mean sum of the surrounding area of the pixel (r, c) minus constant C .

$$Th2 = \begin{cases} 0 & \text{if } Gray(r, c) > T(r, c) \\ \text{maxValue} & \text{otherwise} \end{cases} \quad (8)$$

Where $T(r, c)$ is the adaptive mean threshold value which individually computed as the mean of the surrounding region of that pixel (r, c) minus the C constant. MaxValue is the highest grayscale value is (255). In (9), the pixel intensity threshold is determined, so that the pixel values that are less than 30 are considered as black (0); otherwise, they should be white (1). This is due to the saturation phenomena of human vision.

$$Th3 = \begin{cases} 0 & \text{if } Grayimage(r, c) \leq 30 \\ 1 & \text{otherwise} \end{cases} \quad (9)$$

In (10), the Canny edge detector thresholds steps are calculated to ensure that all-important (real) edges that construct the form of a moving object will be recognized and added properly. However, this process needs a fine-tuning between the image properties to find the correct real edges.

$$Th4 = \text{Canny}(\text{low}, \text{high}, \text{Size} = 3) \quad (10)$$

The pixel is recognized as an edge if its gradient is higher than the upper threshold; the pixel is not an edge if its gradient is less than the lower threshold. The pixel is considered as a real edge if its gradient value ranges between the upper and lower thresholds, in addition to being associated with a pixel that is over the upper threshold. Finally in stage three, the XOR-bitwise accumulation and basic (AND and OR) operations are used to decide which pixels are related to the objects and which are not. In terms of the theoretical contribution, the small details (noisy background pixels) should be omitted as in (11):

$$\text{Result} = \text{XOR}(Th1 \& Th2, Th3 + Th4) \quad (11)$$

where "&" represents an AND-bitwise, "+" is an OR-bitwise, while XOR is an Exclusive-OR (11=0, 00=0, 10=1, 01=1). *Result* represents a resulted image. However, the use of the bitwise gates may need a theoretical view, as the operations should be chosen precisely so that the first two thresholds of Gaussian and mean (Th1, and Th2) are used to extract the object's body pixels actually by stern condition (&), while the thresholds (Th3, and Th4) are used to improve the real edges and object boundaries using tolerant condition (+). The use of XOR-accumulation is to gather the resulted pixels and reject both the noisy background pixels and the misleading results when both Th1 and Th2 is equal to 1 and Th3+Th4 is equal to 1, taking into consideration all possible cases of noise generation. This thought is compatible and measured with the programming practical execution. More explanation upon the practical side and the obtained results are further elaborated in the next section.

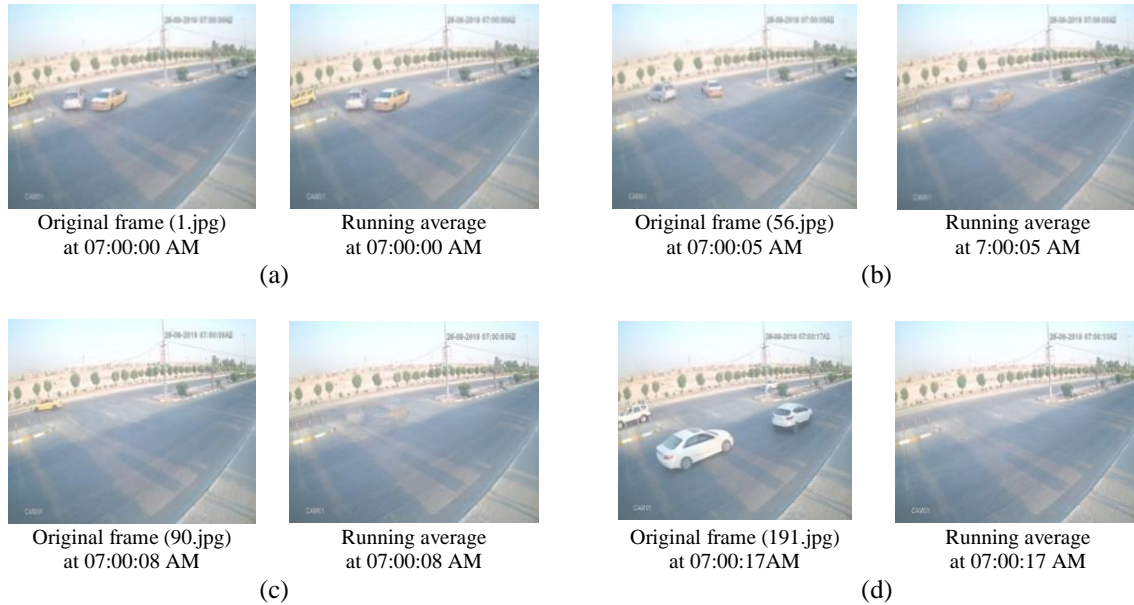


Figure 3. Explanation of running average technique at different time of 11 FPS video from (a) original frame no. 1.jpg, (b) original frame no. 56.jpg, (c) original frame no. 90.jpg, and (d) original frame no. 191.jpg

4. RESULTS AND DISCUSSION

4.1. Images set and ground truth generation

The proposed TAXA algorithm is compared to the most popular available methods on OpenCV library based on high-definition HD resolution videos (high details). HD resolution videos have recently seen as new challenge for surveillance systems processing. The Figures 4(a) to 4(g) show seven frames in different times and conditions (including moving vehicles, waving of trees, dust, sunshine and shadow) for a fixed camera video (1920×1080) used in application and testing.

Based on the following steps, the ground truth is calculated for each frame. Initially, each frame is gray-scale converted. Secondly, object frontiers are manually detected by human observation by precisely recognizing objects as black blocks as in Figures 5(a) and (b). Thirdly, for each frame the canny edge detector is used to detect the true boundaries as in Figure 5(c). Finally, the ground truth frames are produced as in Figure 5(d).

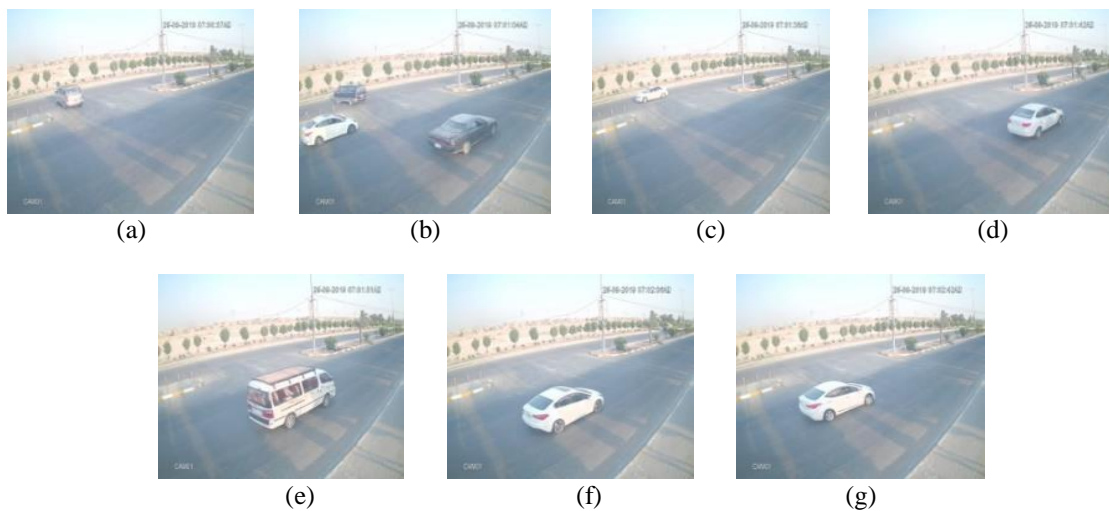


Figure 4. Referenced frames used for the evaluation of HD video at 7:00 am, frame size (1920×1080): (a) scene 1 no. 636.jpg, (b) scene 2 no. 710.jpg, (c) scene 3 no. 1057.jpg, (d) scene 4 no. 1129.jpg, (e) scene 5 no. 1225.jpg, (f) scene 6 no. 1387.jpg, and (g) scene 7 no. 1789.jpg



Figure 5. Ground truth generation, (a) original 710.jpg, (b) convert it to grayscale (black blobs), (c) Canny edge detector applying, and (d) ground truth

4.2. Evaluation results

The results are collected on the basis of the seven source frames presented in Figure 4 and Tables 1 to 3. It is determined based on precision measurement, calculation times, the use of CPU, memory, and the subjective evaluation of all results of tables. The precision ratings are excellent (90...99), very good (80...89), good (70...79), and acceptable (60...69). The Core i7 device has 6 GB storage, and OpenCV version (4.1.25) with Python library (3.7) in PyCharm editor implements each of the proposed TAXA and the alternative algorithms. The average results in following Table 1 show that the proposed TAXA algorithm has achieved a promising result and outputs excellent and highest quality all other prominent algorithms. The proposed TAXA algorithm overrides the others, on the basis of the Table 2 and Figure 6(a) for execution time results, Figure 6(b) for CPU usage results, Figure 6(c) for memory usage results. The proposed algorithm exceeds each of the KNN, GMG and LSBP, according to the time of computations (execution) and is about the like of MOG2 (designed for real time operations). As compared to the ground-truth frames of Table 1, a fair subjective evaluation is showed through understanding and confidences in the results as the original frame No.1225.jpg of in Figures 7(a), the ground truth of scene 5 in Figures 7(b), the TAXA result in Figure 7(c), the MOG2 result in Figure 7(d), the KNN result in Figure 7(e), the GMG result in Figure 7(f), and the LSBP result in Figure 7(g).

Table 1. Precision measurement results of applied algorithms

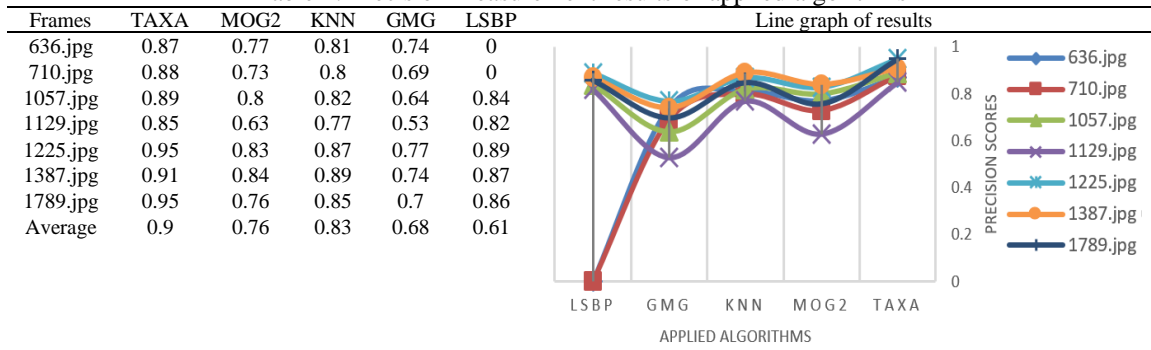


Table 2. Execution times, CPU, and memory usages applied on video length 1:57 minutes, (11 FPS, total of 1297 frames) at 5:37 am, 2560×1920

Measures	TAXA	MOG2	KNN	GMG	LSBP
Execution time/seconds	210	190	213	835	3200
Memory usage	6.56%	11.27%	10.42%	42.76%	34.38%
CPU usage	20.0%	81.3%	80.5%	59.0%	79.2%

Generally, in all used algorithms, the proposed TAXA algorithm has a superior value. It is worth mentioning that the distributing pixels associated with the objects are more apparent than the other white noisy pixels that relate to the background compared to the ground truth frame. The focus should be on the object body only for more reliable results based on the region of interest concept, and to avoid the background FN by eliminating every referenced frame in Figure 4 based on ROI. Therefore, the TAXA algorithm produces new excellent results compared with the rest as in Table 3.

As a result, the proposed TAXA algorithm still has the superiority scores over the others. It is worth noting that our proposed TAXA algorithm has sufficient criteria for identifying the objects' shape in order to extract foreground pixels. Consequently, applying XOR-accumulation for the extracted thresholds leads to the extraction of real foreground objects' pixels rather than background pixels; thereby achieving best results over all prominent used algorithms.

Table 3. Precision measure of applied algorithms to the references frames ROIs of Figure 4

RIOS	TAXA	MOG2	KNN	GMG	LSBP	Line graph of results					
636.jpg (350×350)	0.83	0.77	0.81	0.74	0		<p>PRECISION SCORES</p> <p>APPLIED ALGORITHMS</p>				
710.jpg (1550×450)	0.86	0.73	0.79	0.69	0						
1057.jpg (350×350)	0.89	0.83	0.84	0.64	0.86						
1129.jpg (550×350)	0.84	0.62	0.76	0.52	0.82						
1225.jpg (750×450)	0.97	0.83	0.87	0.76	0.89						
1387.jpg (700×350)	0.96	0.83	0.88	0.74	0.88						
1789.jpg (700×350)	0.96	0.76	0.85	0.70	0.85						
Average results	0.90	0.76	0.82	0.68	0.61						

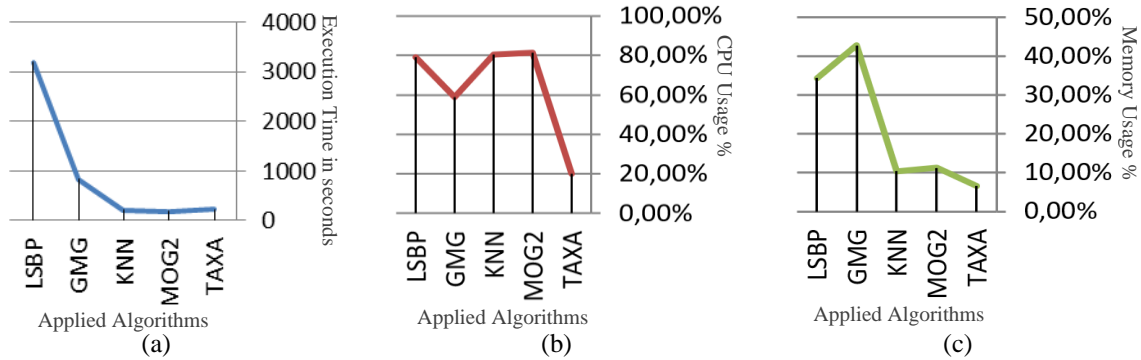


Figure 6. Line chart results of Table 2 (a) time in seconds, (b) CPU usage, and (c) memory usage

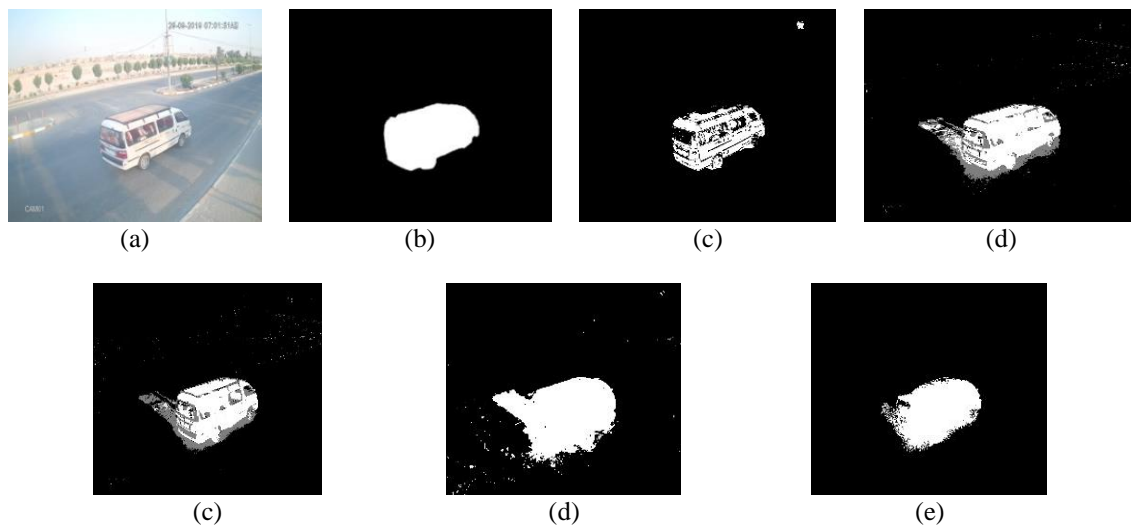


Figure 7. Evaluation of scene (5) frame no. 1225.jpg in Table 1 over algorithms based on ground truth (a) frame no. 1225.jpg, (b) ground truth, (c) TAXA, (d) MOG2, (e) KNN, (f) GMG, and (g) LSBP

5. CONCLUSION

The extraction task for foreground objects is still open and vital to any intelligent surveillance system based on background modelling. This paper proposes a TAXA algorithm, which detection over high definition videos of slow and fast dynamic varied object forms. The TAXA algorithm is new in the application of the XOR-accumulation hypothesis to decide whether it is an object or a history for the pixels. The proposed algorithm works with a hybrid application of median, Gaussian and mean statistical methods over average background and adaptive threshold. In the end, the execution results overcame prominent OpenCV algorithms based on objective measures as well as better subjective assessment. The TAXA algorithm can be used well for object detection surveillance systems. The future work will be to add its code to OpenCV and apply it to real-time applications.

REFERENCES

- [1] R. M. Patil, C. K. P., A. Nasreen, and S. G., "Robust foreground modelling to segment and detect multiple moving objects in videos," *International Journal of Electrical and Computer Engineering (IJECE)*, vol. 10, no. 2, pp. 1337–1345, Apr. 2020, doi: 10.11591/ijece.v10i2.pp1337-1345.
- [2] S. Kumar and J. Sen Yadav, "Video object extraction and its tracking using background subtraction in complex environments," *Perspectives in Science*, vol. 8, pp. 317–322, Sep. 2016, doi: 10.1016/j.pisc.2016.04.064.
- [3] V. Rekha, K. Natarajan, and J. I. Rose, "Foreground algorithms for detection and extraction of an object in multimedia," *International Journal of Electrical and Computer Engineering (IJECE)*, vol. 10, no. 2, pp. 1849–1858, Apr. 2020, doi: 10.11591/ijece.v10i2.pp1849-1858.
- [4] B. Garcia-Garcia, T. Bouwmans, and A. J. Rosales Silva, "Background subtraction in real applications: Challenges, current models and future directions," *Computer Science Review*, vol. 35, p. 100204, Feb. 2020, doi: 10.1016/j.cosrev.2019.100204.
- [5] P. B. Prakoso and Y. Sari, "Vehicle detection using background subtraction and clustering algorithms," *Telecommunication Computing Electronics and Control (TELKOMNIKA)*, vol. 17, no. 3, pp. 1393–1398, Jun. 2019, doi: 10.12928/telkomnika.v17i3.10144.
- [6] H. N. Abdullah and N. H. Abdulghafoor, "Objects detection and tracking using fast principle component purist and kalman filter," *International Journal of Electrical and Computer Engineering (IJECE)*, vol. 10, no. 2, pp. 1317–1326, Apr. 2020, doi: 10.11591/ijece.v10i2.pp1317-1326.
- [7] K. L. Y. Fung *et al.*, "Accurate EELS background subtraction-an adaptable method in MATLAB," *Ultramicroscopy*, vol. 217, p. 113052, Oct. 2020, doi: 10.1016/j.ultramic.2020.113052.
- [8] Y. Xu, H. Ji, and W. Zhang, "Coarse-to-fine sample-based background subtraction for moving object detection," *Optik*, vol. 207, p. 164195, Apr. 2020, doi: 10.1016/j.jjleo.2020.164195.
- [9] W. Zheng, K. Wang, and F.-Y. Wang, "A novel background subtraction algorithm based on parallel vision and Bayesian GANs," *Neurocomputing*, vol. 394, pp. 178–200, Jun. 2020, doi: 10.1016/j.neucom.2019.04.088.
- [10] N. Q. Dung, T. T. T. Duong, T. D. Lam, D. D. Dung, N. N. Huy, and D. Van Thanh, "Corrigendum to 'A simple route for electrochemical glucose sensing using background current subtraction of cyclic voltammetry technique' [J. Electroanal. Chem. 848 (1 September 2019) 113323]," *Journal of Electroanalytical Chemistry*, vol. 855, p. 113600, Dec. 2019, doi: 10.1016/j.jelechem.2019.113600.
- [11] M. S. Zaharin, N. Ibrahim, and T. M. A. Tuan Dir, "Comparison of human detection using background subtraction and frame difference," *Bulletin of Electrical Engineering and Informatics*, vol. 9, no. 1, pp. 345–353, Feb. 2020, doi: 10.11591/eei.v9i1.1458.
- [12] D. Sugimura, F. Teshima, and T. Hamamoto, "Online background subtraction with freely moving cameras using different motion boundaries," *Image and Vision Computing*, vol. 76, pp. 76–92, Aug. 2018, doi: 10.1016/j.imavis.2018.06.003.
- [13] B. S. Y. Lam, A. M. Y. Chu, and H. Yan, "Statistical bootstrap-based principal mode component analysis for dynamic background subtraction," *Pattern Recognition*, vol. 100, p. 107153, Apr. 2020, doi: 10.1016/j.patcog.2019.107153.
- [14] H. Sajid, S.-C. S. Cheung, and N. Jacobs, "Motion and appearance based background subtraction for freely moving cameras," *Signal Processing: Image Communication*, vol. 75, pp. 11–21, Jul. 2019, doi: 10.1016/j.image.2019.03.003.
- [15] G. Srivastava and R. Srivastava, "Salient object detection using background subtraction, Gabor filters, objectness and minimum directional backgroundness," *Journal of Visual Communication and Image Representation*, vol. 62, pp. 330–339, Jul. 2019, doi: 10.1016/j.jvcir.2019.06.005.
- [16] J. L. M. Iqbal and S. Arun, "Intelligent information system for suspicious human activity detection in day and night," *International Journal of Informatics and Communication Technology (IJ-ICT)*, vol. 7, no. 3, pp. 117–123, Dec. 2018, doi: 10.11591/ijict.v7i3.pp117-123.
- [17] Y. Hu, K. Sirlantzis, G. Howells, N. Ragot, and P. Rodríguez, "An online background subtraction algorithm deployed on a NAO humanoid robot based monitoring system," *Robotics and Autonomous Systems*, vol. 85, pp. 37–47, Nov. 2016, doi: 10.1016/j.robot.2016.08.013.
- [18] D. Ortego, J. C. SanMiguel, and J. M. Martínez, "Stand-alone quality estimation of background subtraction algorithms," *Computer Vision and Image Understanding*, vol. 162, pp. 87–102, Sep. 2017, doi: 10.1016/j.cviu.2017.08.005.
- [19] Y.-T. Chan, "Comprehensive comparative evaluation of background subtraction algorithms in open sea environments," *Computer Vision and Image Understanding*, vol. 202, p. 103101, Jan. 2021, doi: 10.1016/j.cviu.2020.103101.
- [20] R. N. Rithesh, R. Vignesh, and M. R. Anala, "Autonomous traffic signal control using decision tree," *International Journal of Electrical and Computer Engineering (IJECE)*, vol. 8, no. 3, pp. 1522–1529, Jun. 2018, doi: 10.11591/ijece.v8i3.pp1522-1529.
- [21] A. F. Abbas, U. ullah Sheikh, F. T. AL-dhief, and M. N. H. Mohd, "A comprehensive review of vehicle detection using computer vision," *TELKOMNIKA (Telecommunication Computing Electronics and Control)*, vol. 19, no. 3, p. 838, Jun. 2021, doi: 10.12928/telkomnika.v19i3.12880.
- [22] P. Ramya and R. Rajeswari, "A modified frame difference method using correlation coefficient for background subtraction," *Procedia Computer Science*, vol. 93, no. September, pp. 478–485, 2016, doi: 10.1016/j.procs.2016.07.236.
- [23] S. Fu, G. Jiang, and M. Yu, "An effective background subtraction method based on pixel change classification," in *2010 International Conference on Electrical and Control Engineering*, Jun. 2010, pp. 4634–4637, doi: 10.1109/ICECE.2010.1120.

- [24] Z. Zivkovic, "Improved adaptive Gaussian mixture model for background subtraction," in *Proceedings of the 17th International Conference on Pattern Recognition, 2004 ICPR 2004*, 2004, vol. 2, pp. 28–31, doi: 10.1109/ICPR.2004.1333992.
- [25] Z. Zivkovic and F. van der Heijden, "Efficient adaptive density estimation per image pixel for the task of background subtraction," *Pattern Recognition Letters*, vol. 27, no. 7, pp. 773–780, May 2006, doi: 10.1016/j.patrec.2005.11.005.
- [26] A. B. Godbehere, A. Matsukawa, and K. Goldberg, "Visual tracking of human visitors under variable-lighting conditions for a responsive audio art installation," in *2012 American Control Conference (ACC)*, Jun. 2012, pp. 4305–4312, doi: 10.1109/ACC.2012.6315174.
- [27] L. Guo, D. Xu, and Z. Qiang, "Background subtraction using local SVD binary pattern," in *2016 IEEE Conference on Computer Vision and Pattern Recognition Workshops (CVPRW)*, Jun. 2016, pp. 1159–1167, doi: 10.1109/CVPRW.2016.148.
- [28] S. R. Hanchinamani, S. Sarkar, and S. S. Bhairannawar, "Design and implementation of high speed background subtraction algorithm for moving object detection," *Procedia Computer Science*, vol. 93, pp. 367–374, 2016, doi: 10.1016/j.procs.2016.07.222.
- [29] B. Farou, M. N. Kouahla, H. Seridi, and H. Akdag, "Efficient local monitoring approach for the task of background subtraction," *Engineering Applications of Artificial Intelligence*, vol. 64, pp. 1–12, Sep. 2017, doi: 10.1016/j.engappai.2017.05.013.
- [30] D. D. Bloisi, A. Pennisi, and L. Iocchi, "Parallel multi-modal background modeling," *Pattern Recognition Letters*, vol. 96, pp. 45–54, Sep. 2017, doi: 10.1016/j.patrec.2016.10.016.
- [31] J. S. H. and L. S., "Detection and tracking of moving object using modified background subtraction and Kalman filter," *International Journal of Electrical and Computer Engineering (IJECE)*, vol. 11, no. 1, pp. 217–223, Feb. 2021, doi: 10.11591/ijece.v11i1.pp217-223.
- [32] M. Amine, K. Djoudi, and I. R. Karas, "A new method for vehicles detection and tracking using information and image processing," *International Journal of Electrical and Computer Engineering (IJECE)*, vol. 11, no. 6, pp. 4942–4949, Dec. 2021, doi: 10.11591/ijece.v11i6.pp4942-4949.
- [33] H. T. Rashid and I. H. Ali, "Multi-camera collaborative network experimental study design of video surveillance system for violated vehicles identification," *Journal of Physics: Conference Series*, vol. 1879, no. 2, p. 22090, May 2021, doi: 10.1088/1742-6596/1879/2/022090.

BIOGRAPHIES OF AUTHORS



Hasan Thabit Rashid Kurmasha    received his PhD degree from University of Babylon in 2021. Currently he is a lecturer in University of Kufa, Najaf, Iraq. His research interests in Intelligent video surveillance systems. He can be contacted at email: hasan.th.kurmasha@student.uobabylon.edu.iq.



Israa Hadi Ali    from 2013 til now in staff of college of information technology, Babylon University, Iraq. Her main areas are video tracking and analysis, image processing, multi-media and information hiding. She can be contacted at email: Israa_hadi1968@yahoo.com.